

We are IntechOpen, the world's leading publisher of Open Access books Built by scientists, for scientists

6,900

Open access books available

186,000

International authors and editors

200M

Downloads

Our authors are among the

154

Countries delivered to

TOP 1%

most cited scientists

12.2%

Contributors from top 500 universities



WEB OF SCIENCE™

Selection of our books indexed in the Book Citation Index
in Web of Science™ Core Collection (BKCI)

Interested in publishing with us?
Contact book.department@intechopen.com

Numbers displayed above are based on latest data collected.
For more information visit www.intechopen.com



Pulsed-Laser Ablation of Au Foil in Primary Alcohols Influenced by Direct Current

Karolína Šišková

*Dept. of Physical Chemistry, RCPTM,
Palacky University in Olomouc
Czech Republic*

1. Introduction

Almost two decades ago, Henglein pioneered the application of laser pulses for the synthesis of nanoparticles (Amendola & Meneghetti, 2009, as cited in Henglein et al., 1993). Since that the pulsed-laser ablation process of a foil performed in liquids is one of the top-down processes of nanomaterials generation. In a nutshell, laser pulses are focused into a metallic target immersed in a particular liquid producing thus nanoparticles dispersions (Amendola & Meneghetti, 2009; Georgiou & Koubenakis 2003; Zhigilei & Garrison, 1999). Noble metal nanoparticles are frequently formed by this approach because of a well-known fact that the as-prepared nanoparticle solutions do not contain any by-products and chemicals remaining from usual bottom-up approaches such as chemical syntheses. Hence, pulsed-laser ablation constitutes a “green” technique of nanoparticles formation.

There are several other benefits which make pulsed-laser ablation process attractive. One of them lies in the choice of ablation medium which is usually determined by a further usage of noble metal nanoparticles. So far, numerous papers have been written about pulsed-laser ablation performed in water and in aqueous solutions of simple ions (e.g. Procházka et al, 1997; Srnová et al, 1998; Šišková et al, 2008), surfactants (e.g. Fong et al, 2010), organic molecules (e.g. Darroudi et al, 2011; Kabashin et al, 2003; Mafune et al, 2002; Šišková et al, 2007, 2008, 2011), or even DNA (Takeda et al, 2005). In the literature, there have also been published pulsed-laser ablation processes of metallic foils performed in ionic liquids (Wender et al., 2011), or in a wide range of organic solvents, such as chloroform (Compagnini et al., 2002; Mortier et al, 2003; Šišková et al, 2010), toluene (Amendola et al., 2005), tetrahydrofurane (Amendola et al., 2007), dimethylsulfoxide (Amendola et al., 2007), N,N-dimethylformamid (Amendola et al., 2007), acetonitrile (Amendola et al., 2007), acetone (Burakov et al., 2005, 2010; Boyer et al., 2010; Tarasenko et al, 2005), primary alcohols (Burakov et al, 2010; Compagnini et al, 2002; Simakin et al, 2004; Werner et al, 2008).

Another substantial advantage of pulsed-laser ablation process is the possibility to choose (at least in principle) laser wavelength, pulse duration (ns, ps, fs), energy per pulse, and fluence (energy per area). All these parameters distinctly influence the final nanoparticles size, shape, uniformity, and their production efficiency. The reader is referred to the appropriate literature for more details, namely concerning the other advantages and

disadvantages of the pulsed-laser ablation process in conjunction with the parameters (e.g. Amendola & Meneghetti, 2009; Franklin & Thareja 2004; Semerok et al., 1999; Sobhan et al., 2010; Tsuji et al., 2004).

Laser pulses can be applied not only for the generation, but also for the size reduction and reshaping of noble metal nanoparticles, the process known as nanoparticles fragmentation (Dammer et al, 2007; Kamat et al., 1998; Kurita et al., 1998; Link et al., 1999; Mafune et al, 2001, 2002; Peng et al., 2005; Shoji et al., 2008; Šmejkal et al., 2003, 2004; Takami et al., 1999; Werner et al., 2010; Yamada et al, 2006, 2007). Laser-pulses induced nanoparticles fragmentation has been described by two possible mechanisms so far: (i) coulomb explosion due to the sequential photo-ejection of electrons during the absorption of a single laser pulse (Link & El-Sayed, 2003; Yamada et al., 2006), and/or (ii) vaporization of particles due to the heating, induced by photon absorption, to a temperature higher than the boiling threshold (Franklin & Thareja 2004; Inasawa et al., 2006; Kurita et al., 1998; Takami et al., 1999). Similarly as in the case of pulsed-laser ablation process, particles fragmentation strongly depends on laser wavelength, pulse duration (ns, ps, fs), energy per pulse, and fluence. For instance, Au nanoparticles with the maximum of extinction at 520 nm can be efficiently fragmented by using the nanosecond laser pulses of 532 nm wavelength using reasonable values of fluence (Amendola & Meneghetti, 2009).

In the past three decades, nanoparticles have gained an increasing attention due to their unique optical, electrical, and magnetic properties which differ from bulk materials (Roduner, 2006). In particular, it has been demonstrated that noble metal nanoparticles (Ag, Au, Cu) possess surface plasmons which are responsible for enhanced light scattering and absorption (Le Ru & Etchegoin, 2008). This characteristic property of noble metal nanoparticles is fully exploited in surface-enhanced Raman scattering (SERS) spectroscopy. Recently, noble metal nanoparticles have also been employed in cancer diagnosis and therapy (Jain et al., 2007) as well as in photovoltaic devices (Atwater, H.A. & Polman A., 2010; Kim et al., 2008; Morfa et al., 2008; Tong et al. 2008).

According to a particular exploitation, either liquid dispersions of nanoparticles, or nanoparticles deposited on a substrate are preferentially required. Noble metal nanoparticles can be deposited on a particular substrate by several different ways depending on the force which is responsible for nanoparticles assembling. Roughly divided, nanoparticles assembling can be directed by molecular interactions, or by external fields as reviewed in more details in (Grzelczak et al., 2010). An elegant method is to allow self-assembling of nanoparticles exploiting spontaneous processes (Rabani et al., 2003; Siskova et al., 2011).

When molecular interactions are intended to be exploited for nanoparticles assembling, either substrate or nanoparticles have to be suitably modified by a surface modifier which enables the mutual interaction between nanoparticles and substrates. As an excellent example, the modification by amino- and/or mercapto-alkylsiloxane, or porphyrins can be referenced (Buining et al., 1997; Doron et al., 1995; Grabar et al., 1996; Šloufová-Srnová & Vlčková, 2002; Sládková et al., 2006). Obviously, surface modifications may be useful in or, on the contrary, disable some applications because they change electrical and optical properties of nanoparticles as well as of substrates (Carrara et al., 2004; de Boer et al., 2005; Durston et al., 1998; Rotello, 2004; Schnippering et al., 2007; Wu et al., 2009). Therefore, many research groups look for other types of nanoparticles assembling. One of many

possibilities is the electrophoretic deposition technique which is based on the fact that charged nanoparticles are driven to and deposit on a substrate's surface when an electric field is applied perpendicular to the substrate (Zhitomirsky et al., 2002).

Recently, a few papers have appeared using electrophoresis for the deposition of noble metal nanoparticles on substrates intended for particular purposes. ZnO nanorod arrays have been decorated by electrophoretically deposited Au nanoparticles (He et al., 2010). Such Au nanoparticle-ZnO nanorod arrays have exhibited an excellent surface-enhanced Raman scattering performance and enabled the detection at a single molecule level (He et al., 2010). Another electrophoretic deposition of Au nanoparticles performed in acetone has been motivated by the effort to prepare a SALDI (surface-assisted laser desorption ionization) substrate (Tsuji et al., 2011). Kim and co. used electrodeposited Au nanoparticles for electrochromic coloration (Nah et al., 2007). In another study (Yang et al., 2009), it has turned out that electrophoresis carried out for a long time (14 hours) can even lead to a preferential growth of nanoparticles on a substrate resulting in nanoplates. By changing the parameters of electrophoresis, namely the current density, the morphologies and structures of the obtained films can be easily controlled and tuned (Yang et al., 2009).

This chapter deals with Au nanoparticles prepared by pulsed-laser ablation process exploiting nanosecond laser pulses of 532 nm wavelength, performed in primary alcohols while direct current passes simultaneously through the ablation medium. Due to the charges present on the surface of arising Au nanoparticles, they are moved toward electrodes where they deposit. We assume the impact of simultaneous electrophoresis on the outcomes of pulsed-laser ablation, i.e., on the resulting nanoparticles dispersions. This point has never been addressed yet. Although electrophoresis of nanoparticles formed by pulsed-laser ablation process, however, using femtosecond laser pulses and aqueous environment, have been investigated by Barcikowski group (Menendez-Manjon et al., 2009), the authors focussed mainly on the velocities of nanoparticles using laser scattering velocimetry and on the surface patterning of metal target induced by the impact of a train of femtosecond laser pulses. In contrast, a complete characterization of Au nanoparticles solutions gets attention in this chapter.

Moreover, the chapter reports brand new results concerning not only the as-prepared solutions of Au nanoparticles influenced by direct current, but also microscopic and spectroscopic characteristics of three selected types of substrates which Au nanoparticles are deposited on due to electrophoresis.

Last, but not least, a possible elucidation of the influence of direct current value on the mechanism of Au nanoparticles generation by the pulsed-laser ablation process combined with electrophoretic deposition and performed in primary alcohols is suggested.

2. Experimental

2.1 Materials

Ethanol and butanol of UV-spectroscopy grade purchased from Fluka were used. Cleaning of a pure Au foil (99.99%, Aldrich) and ablation cell by washing in piranha solution ($\text{H}_2\text{O}_2:\text{H}_2\text{SO}_4$, 1:1) was carried out. The latter was also washed with aqua regia ($\text{HNO}_3:\text{HCl}$, 1:3) in order to remove any residual Au nanoparticles from the previous experiments. Indium-tin-oxide (ITO) and fluorine-tin-oxide (FTO) coated glass substrates purchased from Aldrich were ultrasonicated in acetone (p.a., Penta) and dried by nitrogen flow prior to their use as electrodes in the course of the simultaneous pulsed-laser

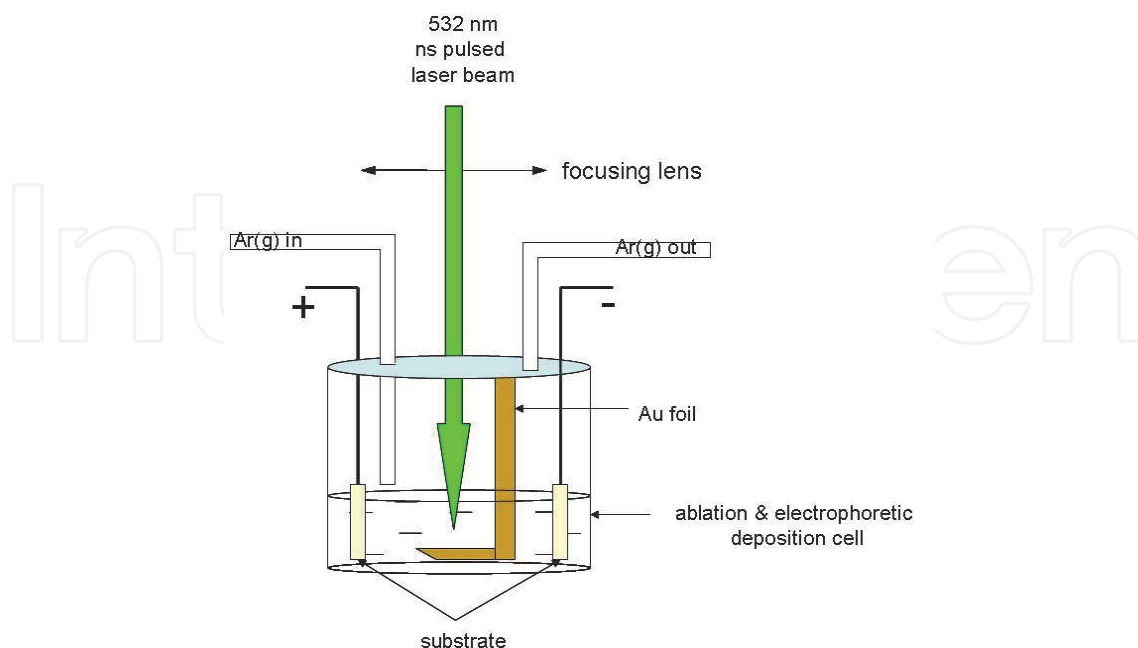
ablation and electrophoretic deposition process. Alternatively, freshly cleaved highly oriented pyrolytic graphite plates (HOPG, purchased from RMI, Lazne Bohdanec, Czech Republic) were employed as electrodes.

2.2 Simultaneous pulsed-laser ablation and electrophoretic deposition

Homemade experimental setup for the simultaneous pulsed-laser ablation and electrophoretic deposition process is depicted in Scheme 1. Cylindrical glass ablation cell with a teflon cover was equipped with (i) two glass tubes allowing inert gas (Ar, 99.999%) to come in and leave, (ii) two electrode holders connected with a power supply, and (iii) a Au foil holder. Inert atmosphere is employed in order to increase the yield of nanoparticles which has been demonstrated in the literature (Werner et al., 2008). Laser pulses provided by Q-switched Nd/YAG laser system (Continuum Surelite I), wavelength 532 nm (the second harmonic) with the repetition rate of 10 Hz, effective diameter of a pseudo-Gaussian spot of 5 mm, and pulse width (FWHM) of 6 ns were used for the pulsed-laser ablation of the Au foil immersed in primary alcohols (100 mL). Pulsed-laser beam passed through ca. 8 mm column of a primary alcohol solution before hitting the Au target. Lenses (plano-convex, BK7, 25 mm in diameter) of 250 mm focal length were used to focus the pulsed-laser beam. The Au foil was irradiated for 6 min by a train of laser pulses of the 105 mJ/pulse energy as determined by a volume absorber powermeter PS-V-103 (Gentec Inc.). Simultaneously with the pulsed-laser ablation, electrophoresis took place, i.e. direct electric current (controlled by an ampere-meter) passed through the ablation medium due to the immersed electrodes (3 cm distant). Two values of direct current were employed, 10 μ A and 17 μ A (the applied voltage was set accordingly). The experiments have been performed at least 3 times.

2.3 Instrumentation

UV-visible extinction spectra of Au nanoparticle solutions in a 1 cm cuvette as well as of the selected substrates with electrophoretically deposited Au nanoparticles were recorded on a



Scheme 1. Depiction of experimental setup for simultaneous pulsed-laser ablation and electrophoresis.

double-beam spectrophotometer (Perkin-Elmer Lambda 950). Zeta-potentials were measured by means of Zetasizer Nano series (Malvern Instruments). Transmission electron microscopy (TEM) was used for the characterization of sizes of Au nanoparticles dispersed in alcoholic solutions after the simultaneous pulsed-laser ablation and electrophoresis. TEM imaging of dried drops of the Au nanoparticle solutions deposited on a carbon-coated Cu grid was performed using a JEOL-JEM200CX microscope. Scanning electron microscopy (SEM) was employed for the characterization of ITO- and/or FTO-coated glass substrates. SEM images were recorded on a SEM microscope Quanta 200 FEI. HOPG substrates were measured on Ntegra scanning tunnelling microscope (STM). Mechanically clipped Pt/Ir tip was approached toward a sample until a set tunnel current was detected. All STM experiments were done under ambient conditions. STM images were recorded and treated by using Nova 1.0.26 software provided by NT-MDT.

3. Results and discussion

Our choice of Au target, primary alcohols, and the other parameters for the combined pulsed-laser ablation and electrophoretic deposition (PLA+EPD) process has been influenced by several good reasons. First of all, Au nanoparticles are preferred by many applications as it has been well documented in Introduction. Furthermore, they do not undergo surface oxidation as easily as Ag and/or Cu nanoparticles (Muto et al., 2007). Primary alcohols as ablation medium have been chosen because of a good stability of Au nanoparticles in ethanol and other aliphatic alcohols as reported in the literature many times (Amendola et al., 2006, 2007; Amendola & Meneghetti, 2009; Compagnini et al., 2002, 2003). Laser pulses of nanosecond time duration have been rather used because the occurrence of explosive boiling or other photomechanical ablation mechanisms is suppressed in comparison to the situation when using femtosecond pulses (Amendola & Meneghetti, 2009). The 532 nm wavelength has been employed in our study owing to the fact that a narrow particle size distribution can be obtained due to an efficient Au nanoparticles fragmentation accompanying their generation (by pulsed-laser ablation) at this wavelength. The selection of substrate types serving as electrodes is given by possible applications of Au nanoparticles-modified substrates in photovoltaic devices. Therefore, indium-tin-oxide (ITO) and/or fluorine-tin-oxide (FTO) coated glass substrates have been used. On the contrary, highly oriented pyrolytic graphite (HOPG) plates serving as electrodes in the PLA+EPD process have been employed with the aim to investigate the influence of the surface roughness on the character of electrodeposited Au nanoparticles, thus, HOPG has been chosen for a purely scientific reason.

3.1 Au nanoparticles solutions resulting from PLA+EPD process

In general, Au nanoparticles possess surface plasmon (collective oscillations of free electrons) resonances in the visible region of the electromagnetic spectrum. The position of the maximum of surface plasmon extinction (i.e., absorption + scattering) strongly depends on the nanoparticle size, shape, surrounding, and aggregation state (Rotello, 2004). Thus, measurements of extinction spectra of Au nanoparticle dispersions can serve as a first tool of their characterization. However, this characterization is insufficient since it does not report solely about one feature of nanoparticles. Therefore, transmission electron microscopy (TEM) has to be used as well in order to visualize Au nanoparticles and to distinguish

between influences of shape and/or size on extinction spectrum for instance. Another important feature of nanoparticles in solutions is their zeta-potential which enables to predict their stability in solutions, their aggregation state. Obviously, the combination of all three measurements can fully characterize the Au nanoparticle alcoholic solutions resulting from the PLA+EPD process.

Figure 1 shows UV-visible extinction spectra of Au nanoparticles generated by the PLA+EPD process in ethanol. Two distinct values of direct current, 10 and 17 μA , have been allowed to pass through the ethanolic ablation medium. These Au nanoparticles solutions are labelled from now on as Au10 and Au17 according to the passing direct current values.

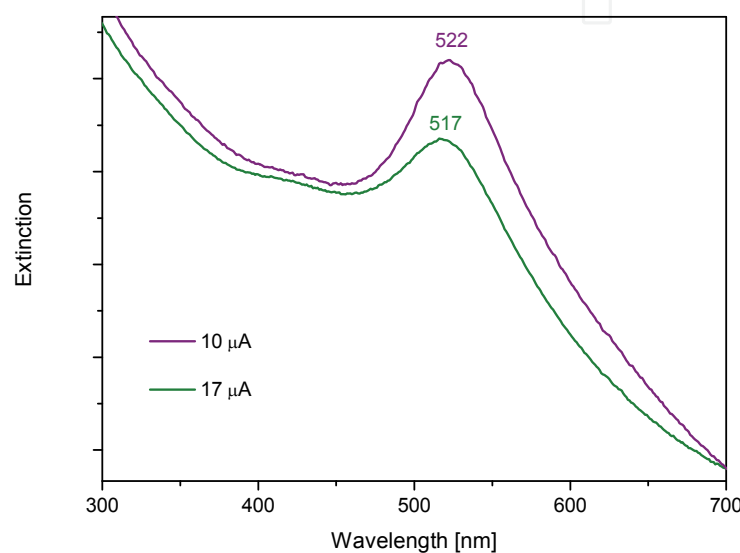


Fig. 1. UV-vis extinction spectra of Au nanoparticles generated by PLA+EPD process in ethanol while direct current of 10 μA and/or 17 μA passed through.

The maximum of surface plasmon extinction of Au10 is located at 522 nm, while that of Au17 is placed at 517 nm - Figure 1. Considering that all the other conditions, except for the direct current value, are the same (duration of PLA+EPD, laser fluence, experimental setup, etc.), and taking into account Mie theory (Rotello, 2004), the average nanoparticle size of Au17 could be smaller than that of Au10. This assumption is corroborated by particle size distribution (PSD) determined on the basis of TEM imaging - Figure 2. While Au10 contains the nanoparticles of 7.3 ± 3.1 nm in diameter (Figures 2A,B), nanoparticles of 4.0 ± 0.9 nm in diameter are encountered in Au17 (Figures 2C,D).

Interestingly, the optical density of Au10 is slightly higher than that obtained for Au17 (Figure 1) which can be related to a lower concentration of nanoparticles in Au17 solution. The decrease of Au nanoparticles concentration in Au17 solution is most probably caused by a higher amount of electro-deposited Au nanoparticles on electrode surface when the direct current of 17 μA is passed through the ablation medium. This hypothesis will be discussed in the next section.

Zeta potentials of Au nanoparticles ethanolic solutions have been measured and are presented in Table 1. Both types of solutions, Au10 and Au17, reveal values below -30 mV which indicates stable nanoparticle dispersions.

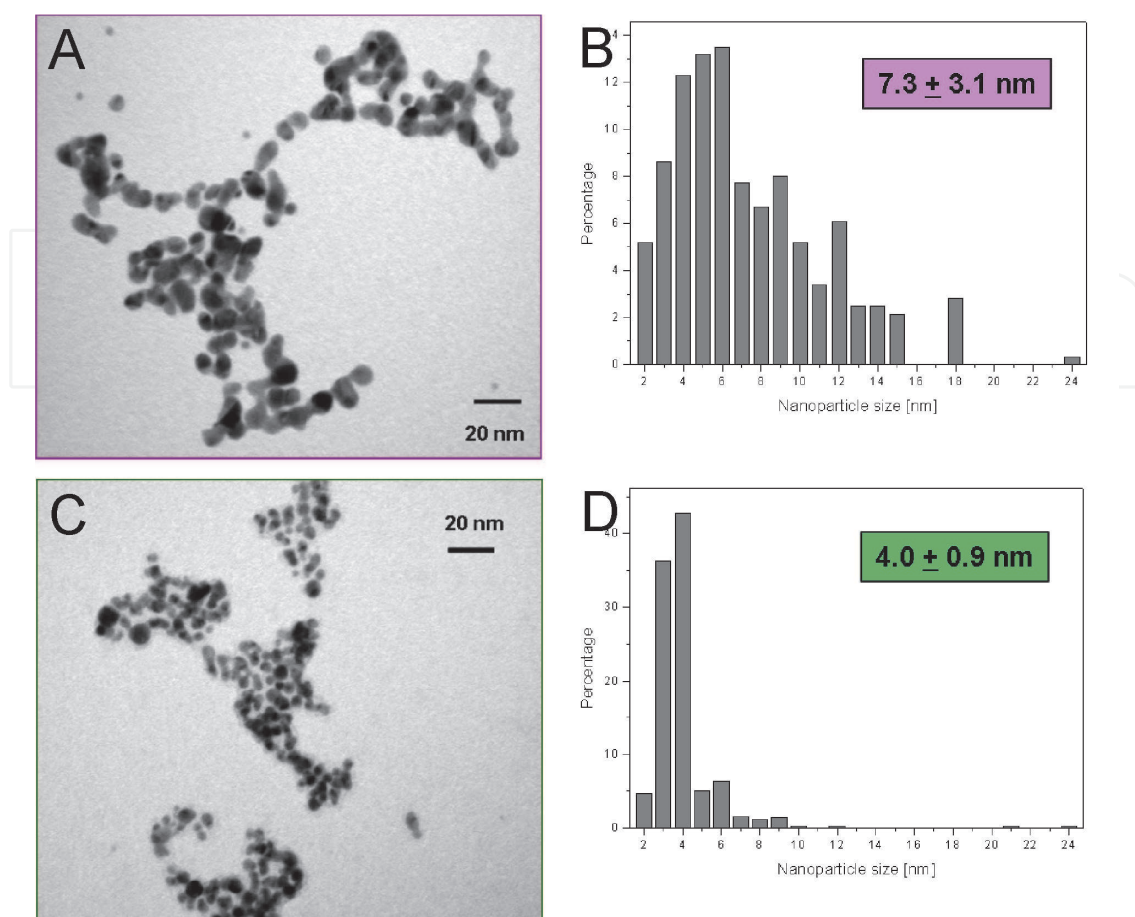


Fig. 2. TEM images (A, C) and appropriate PSD (B, D) of Au nanoparticles formed by PLA+EPD process while 10 μA (A, B) and/or 17 μA (C, D) passing through ethanolic ablation medium.

System label	Solvent	DC [μA]	Zeta potential [mV]
Au10	Ethanol	10	-37.4 ± 2.0
Au17	Ethanol	17	-42.6 ± 0.8
Au10B	Butanol	10	-10.8 ± 1.1
Au17B	Butanol	17	-12.9 ± 1.2

Table 1. Zeta potentials determined for ethanolic as well as butanolic Au nanoparticle solutions. DC means direct current.

In the next step, the PLA+EPD process has been performed in butanol. The resulting Au nanoparticles solutions are entitled as Au10B and Au17B when direct current of 10 μA and 17 μA passed through the butanolic ablation medium, respectively. The values of zeta potentials of these systems are presented in Table 1. They indicate rather unstable Au nanoparticles solutions since the values are above -30 mV and below 30 mV. The differences in zeta potential values of Au10, Au17, and Au10B, Au17B can be ascribed to different

dielectric constants of solvents: ethanol possess the value of 24.3, while butanol 17.1 (Sýkora, 1976).

UV-visible extinction spectra of Au10B and Au17B solutions are shown in Figure 3. Both systems manifest themselves by a well pronounced surface plasmon extinction band with the maximum located at 526 nm indicating thus similar sizes of Au nanoparticles. This idea has been confirmed by PSD based on TEM imaging, presented in Figure 4. Au nanoparticles in Au10B solution reveal sizes of 4.9 ± 1.2 nm and in Au17B sizes of 5.2 ± 1.7 nm in diameter.

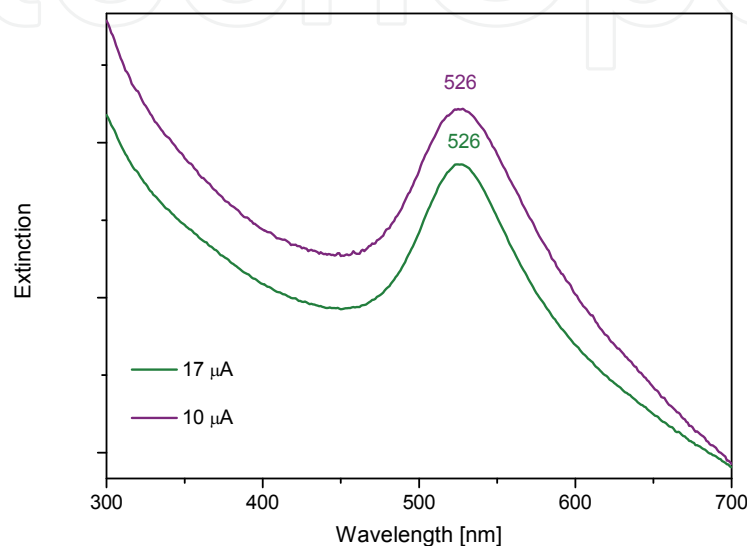


Fig. 3. UV-vis extinction spectra of Au nanoparticles generated by PLA+EPD process in butanol while direct current of 10 μ A and/or 17 μ A allowed to pass through.

Similarly as in the case of ethanolic Au nanoparticle solutions, the concentrations of Au nanoparticles appear to be slightly higher in Au10B than in Au17B solution. The reason will be discussed in the next section.

To sum up, it can be concluded that Au nanoparticles of controlled sizes dispersed in ethanol can be prepared by changing the direct current passing through the ethanolic ablation medium during the PLA+EPD process. In contrast, the same factor (direct current value) does not induce any changes in the average size of Au nanoparticles when formed by the PLA+EPD process in butanol. Considering the zeta potential values of ethanolic and butanolic Au nanoparticles solutions, this result is fully understandable since the higher the zeta potential value, the stronger effect of applied electric field on the generated nanoparticles. The longer aliphatic chain of butanol induces smaller zeta potential values of generated Au nanoparticles and, consequently, the effect of direct current passing during the PLA+EPD process is decreased.

Furthermore, ethanolic Au nanoparticles solutions can be prepared with a narrower particle size distribution when the direct current of 17 μ A instead of 10 μ A employed. On the contrary, the dispersity of butanolic Au nanoparticles solutions is almost negligibly influenced. Obviously, the length of primary alcohols has a distinct effect on the average size of Au nanoparticles generated by the PLA+EPD process.

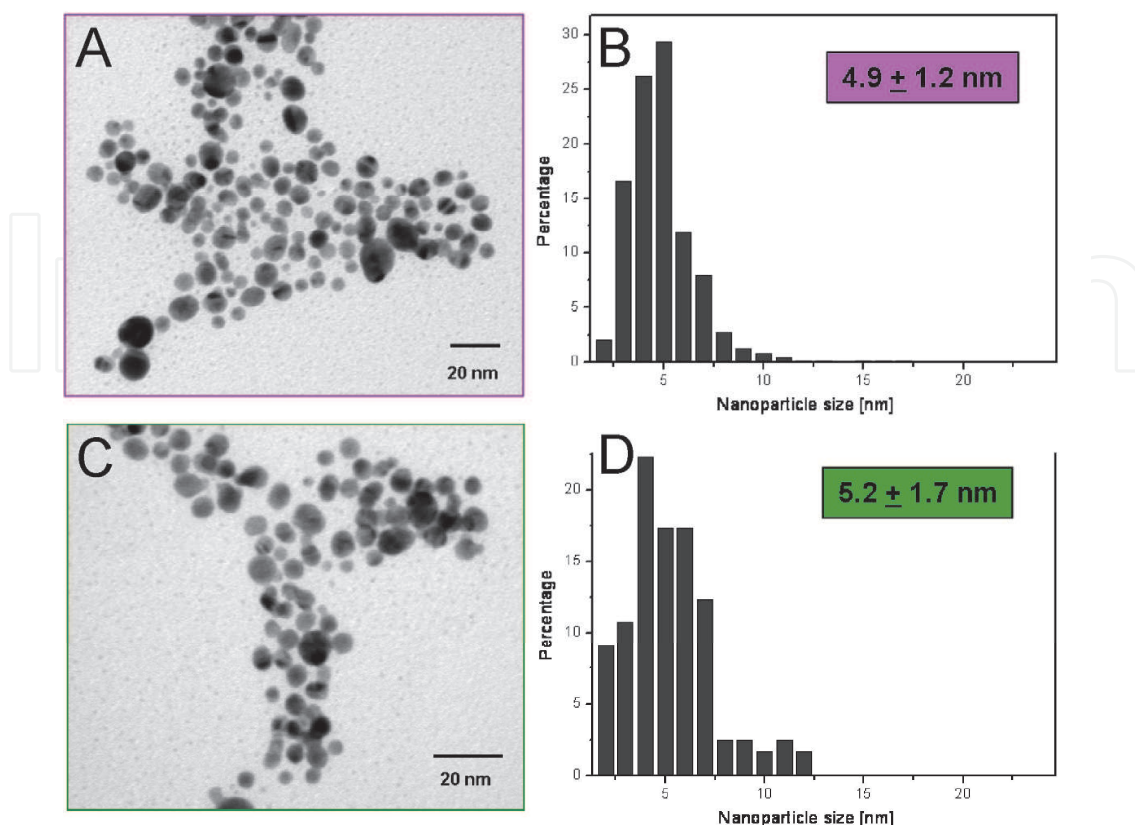


Fig. 4. TEM images (A, C) and appropriate PSD (B, D) of Au nanoparticles formed by PLA+EPD process while 10 μ A (A, B) and/or 17 μ A (C, D) passing through butanolic ablation medium.

3.2 Substrates with electrophoretically-deposited Au nanoparticles

In this section, three types of substrates serving as electrodes in the PLA+EPD process will be characterized by means of microscopic techniques and visible absorption spectroscopy. With respect to the negative values of zeta potential of generated Au nanoparticles in both primary alcohols, they are preferentially deposited on anodes.

3.2.1 ITO-coated glass substrates

SEM images of the ITO-coated glass substrates modified by electrodeposited Au nanoparticles during the PLA+EPD process performed in ethanol are shown in Figure 5. Comparing the SEM images of substrates in Figure 5A (10 μ A direct current) and 5B (17 μ A direct current), a higher surface coverage of substrates by Au nanoparticles is observed at higher current values than at the lower one. This microscopic observation goes hand in hand with the fact deduced from the UV-visible extinction spectra of Au nanoparticles solutions (discussed in the previous section): the final concentration of Au17 solution is lower than that of Au10 solution. The reason for this difference lies in a larger amount of Au nanoparticles being deposited under the higher than the lower current value and, as a consequence, a decrease of Au nanoparticles concentration in Au17 solution being determined.

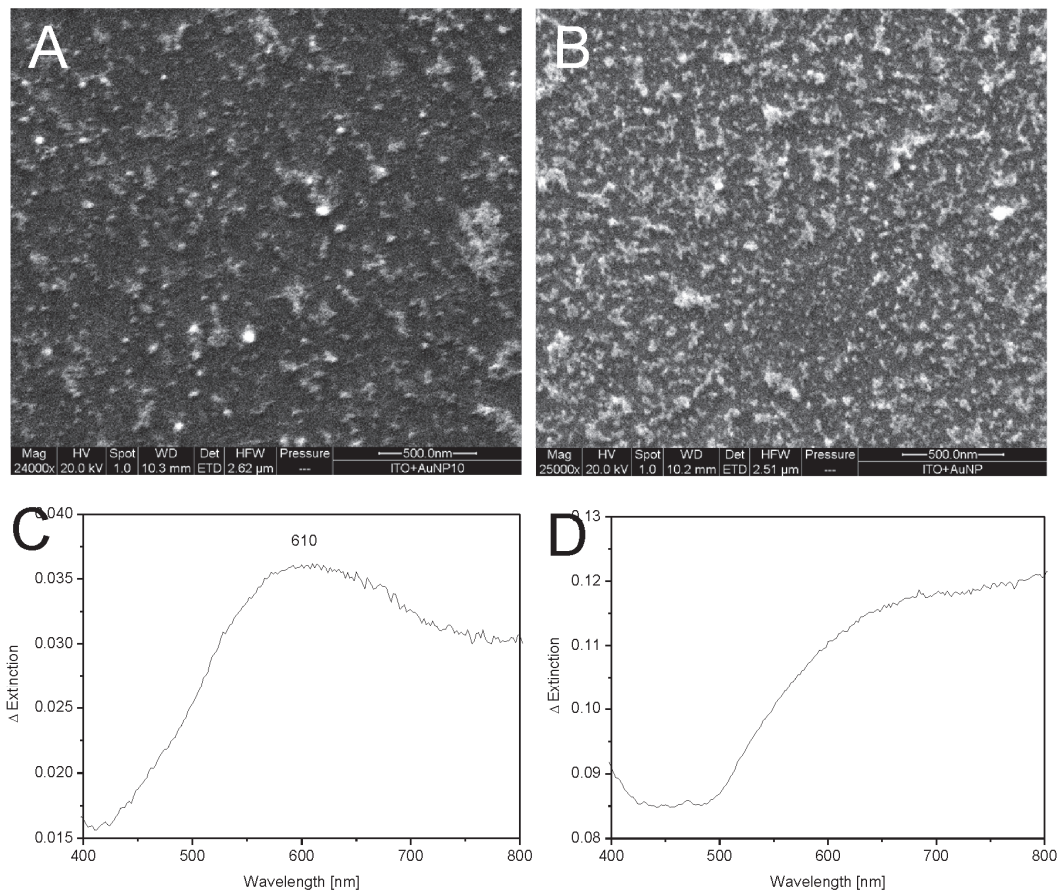


Fig. 5. SEM images (A, B) and particular differential visible extinction spectra (C, D) of ITO-coated glass substrates modified by Au nanoparticles electrodeposited at 10 μA (A, C) and/or 17 μA (B, D) during PLA+EPD process performed in ethanol.

Furthermore, Au nanoparticle aggregates are frequently encountered under both direct current values (Figures 5A and 5B). The aggregation can be also derived from the measured visible extinction spectra of the two discussed substrate samples, presented in Figure 5C and 5D. The differential extinction spectra have been obtained by the subtraction of the extinction spectrum of an unmodified ITO-coated glass substrate from that of a nanoparticles-modified ITO-coated glass substrate. The position of the maximum located at around 610 nm (Figure 5C) reports about aggregated Au nanoparticles on the substrates modified under 10 μA . In the case of Au nanoparticles deposited on ITO-coated glass substrates under 17 μA , there is even no distinct maximum of extinction band (Figure 5D) indicating thus an extensive aggregation of Au nanoparticles.

The same type of experiments using ITO-coated glass substrates as electrodes in the PLA+EPD process has been performed in butanol. The resulting SEM morphologies and differential visible extinction spectra are shown in Figure 6. Comparing Figures 6A (10 μA direct current) and 6B (17 μA direct current), a slightly higher amount of Au nanoparticles can be seen on ITO-coated glass substrates when a higher current value used. This is quite similar result to that observed in ethanolic systems. However, regarding the absolute counts of electro-deposited Au nanoparticles, the substrates from ethanolic solutions are generally

more covered by Au nanoparticles than that obtained in butanolic solutions. As it has been already stated above, the higher zeta potential values of Au nanoparticles in ethanolic solutions are most probably responsible for this result. Furthermore, Au nanoparticles are more evenly dispersed on ITO-coated glass substrates immersed in butanolic than in ethanolic solutions. This can be related to the effect of aliphatic chain length.

The differential extinction spectra, shown in Figures 6C and 6D, reveal a distinct band with the maximum positioned at 575 nm when the lower, and at 615 nm when the higher current values employed. The positions of the maxima of surface plasmon extinction bands correlate with the microscopic observation presented in Figures 6A and 6B. Indeed, the higher the surface coverage of substrates by Au nanoparticles, the more intense and red-shifted surface plasmon extinction observed. In comparison to the extinction spectra of substrates immersed in ethanolic solutions during the PLA+EPD process, the surface plasmon extinction band is well-developed at both current values exploited for the PLA+EPD process performed in butanol. Thus, regarding the aggregation of Au nanoparticles electro-deposited on ITO-coated glass substrates, it is less pronounced in butanolic than in ethanolic samples. Again, the same result evidenced by two independent methods, microscopic and spectroscopic one.

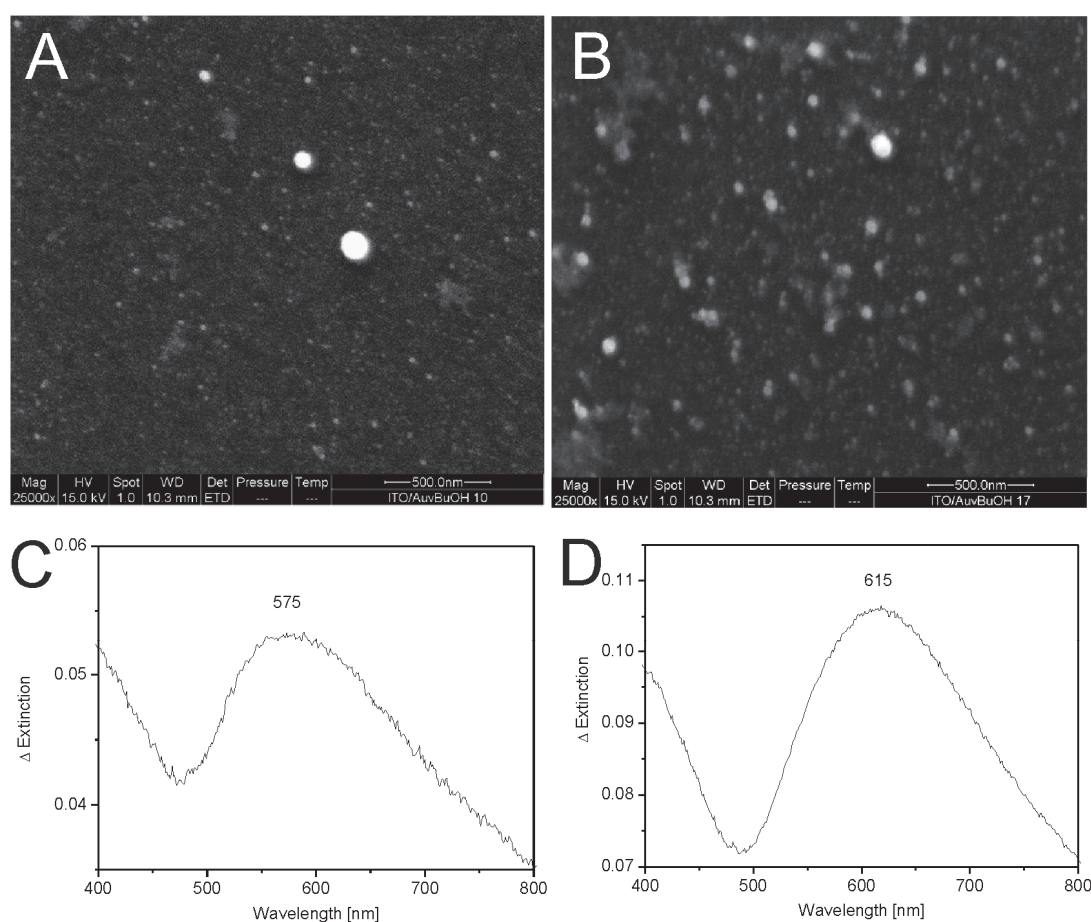


Fig. 6. SEM images (A, B) and particular differential visible extinction spectra (C, D) of ITO-coated glass substrates modified by Au nanoparticles electro-deposited at 10 μ A (A, C) and/or 17 μ A (B, D) during PLA+EPD process performed in butanol.

3.2.2 FTO-coated glass substrates

As it has been already evidenced in the previous section, there are strong effects of direct current value and the type of alcohol on the final coverage of a substrate by Au nanoparticles. In order to investigate if there is any additional influence of substrate roughness, FTO-coated glass substrates have been used as electrodes during the PLA+EPD process performed in ethanol at both values of direct current, 10 μA as well as 17 μA .

In Figure 7A, the SEM image of a cleaned bare FTO-coated glass substrate surface is shown. Obviously, the surface of a FTO-coated glass substrate is very rough with plates and crystals being of sizes of hundreds of nanometers. Taking into account that the local current density can be very different on the edges of a plate and/or crystal, an inhomogeneous distribution of Au nanoparticles and their aggregates on FTO-coated glass substrate can be awaited. Figures 7B and 7C depict the SEM images of Au nanoparticles-modified FTO-coated glass substrates when the lower and the higher electric field applied, respectively. Mutually

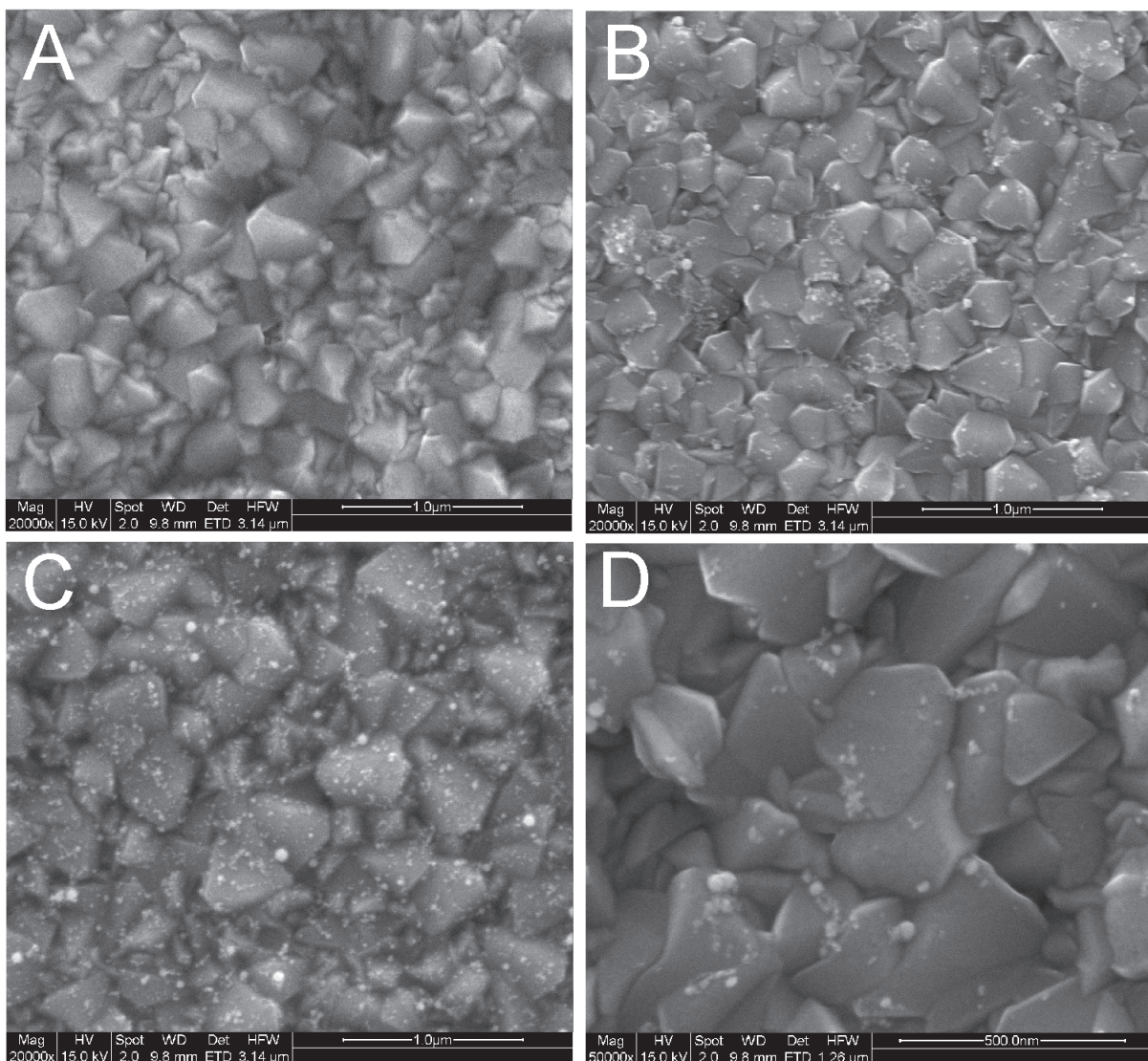


Fig. 7. SEM images of (A) cleaned bare FTO-coated glass substrate, (B, D) Au nanoparticles-modified FTO-coated glass substrate when 10 μA allowed to pass through the ethanolic ablation medium, and (C) Au nanoparticles-modified FTO-coated glass substrate when 17 μA used. Higher magnification is intentionally shown in (D).

compared, there is seen the effect of the direct current value, i.e., with an increasing current a higher surface coverage by Au nanoparticles is observed. When compared to ITO-coated glass substrates serving as electrodes under otherwise the same experimental conditions (SEM images presented in Figures 5A and 5B), the surface of FTO-coated glass substrates is covered even more randomly by Au nanoparticles and their aggregates. These results indicate that the surface roughness of a substrate does play an important role in the course of electrophoretic deposition of Au nanoparticles. The assumption about the inhomogeneity of electric field, made a few lines above, is well documented by a characteristic SEM image in Figure 7D revealing a preferential deposition of Au nanoparticles on the edges of plates and crystals of a FTO-coated glass substrate.

3.2.3 HOPG substrates

Considering the results of the two previous sections, it can be hypothesized that a substrate with a very smooth surface, such as HOPG for instance, could lead to homogeneously dispersed electrodeposited Au nanoparticles since the current density will be homogeneous everywhere on the substrate surface. In order to prove this hypothesis, the PLA+EPD process performed in ethanol while 17 μA passed through has been chosen because under these conditions, the highest degree of aggregation of electrodeposited Au nanoparticles and inhomogeneity in surface coverage were observed as shown in the two previous sections. With respect to the fact that Au nanoparticles in the selected system are tiny (around 4 nm in diameter), another microscopic technique than SEM has to be employed in order to visualize isolated nanoparticles on HOPG substrates. Scanning electron microscopy (STM) can fulfil this task when appropriate measuring conditions met (Durston et al., 1998; Wang et al., 2000).

Figure 8 shows topographic as well as tunnelling current images of a freshly cleaved HOPG surface without and with electrodeposited Au nanoparticles. Smoothness of HOPG surface is well evidenced in Figure 8A where the value along z axis (perpendicular to the plane of the image) stays well below 1 nm. The values of tunnelling current below 0.2 pA have been recorded on a freshly cleaved HOPG substrate measured under ambient conditions, in air and at the room temperature – Figure 8B. Under the same conditions, STM measurements of a HOPG substrate which served as the anode during the PLA+EPD process have been undertaken and one of the resulting topographic images together with its tunnelling current values are shown in Figures 8C and 8D, respectively. Evidently, isolated Au nanoparticles are randomly, however, quite homogeneously dispersed on the surface of a HOPG plate (Figure 8C), the value of 6 nm along z axis is not surpassed. It is worth noting that tunnelling current exceeds 0.4 nA (Figure 8D), which is the value of more than three orders of magnitude higher than on a bare HOPG substrate (Figure 8B). This can be related to the presence of Au nanoparticles.

It is known that HOPG substrate can contain terraces and steps as observed in Figure 8C. Hypothetically, the edges of these terraces and steps could be the places of a locally higher electrical density, hence, more electrodeposited Au nanoparticles could be awaited to occur on these edges. However, this was not the case as evidenced in Figure 8C.

Figure 9 shows topography and tunnelling current image of a smaller flat surface area (200 x 200 nm²) on a HOPG substrate decorated with electrodeposited Au nanoparticles. At this place it should be noticed that the bias voltage of +0.1 V has been applied between the measured HOPG substrate and the tip during STM imaging. This is a sufficiently low value to suppress any unwanted manipulation of Au nanoparticles (Durston et al., 1998).

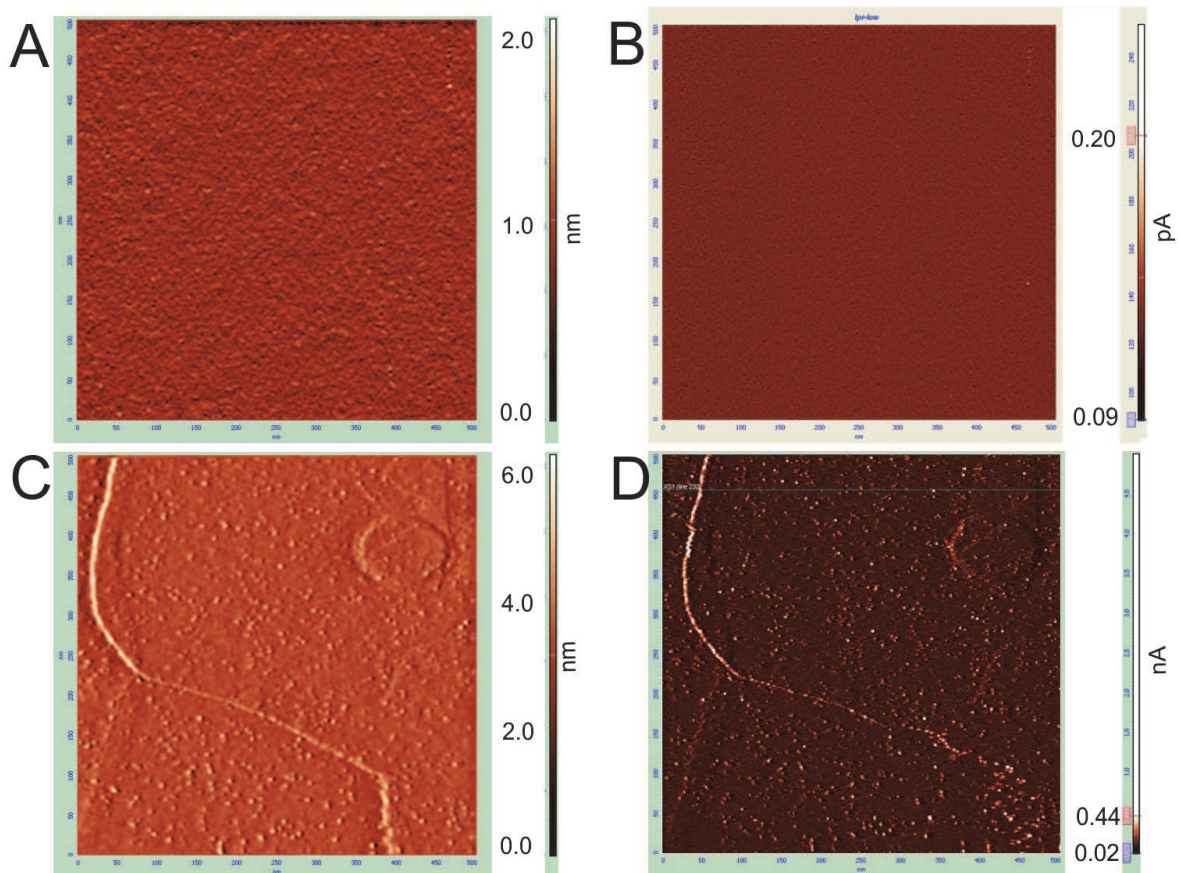


Fig. 8. Topographic (A, C) and tunnelling current (B, D) images of HOPG substrate serving as cathode (A, B) or anode (C, D) in PLA+EPD process while $17 \mu\text{A}$ passed through ethanolic ablation medium. Dimensions of scans are $500 \times 500 \text{ nm}^2$.

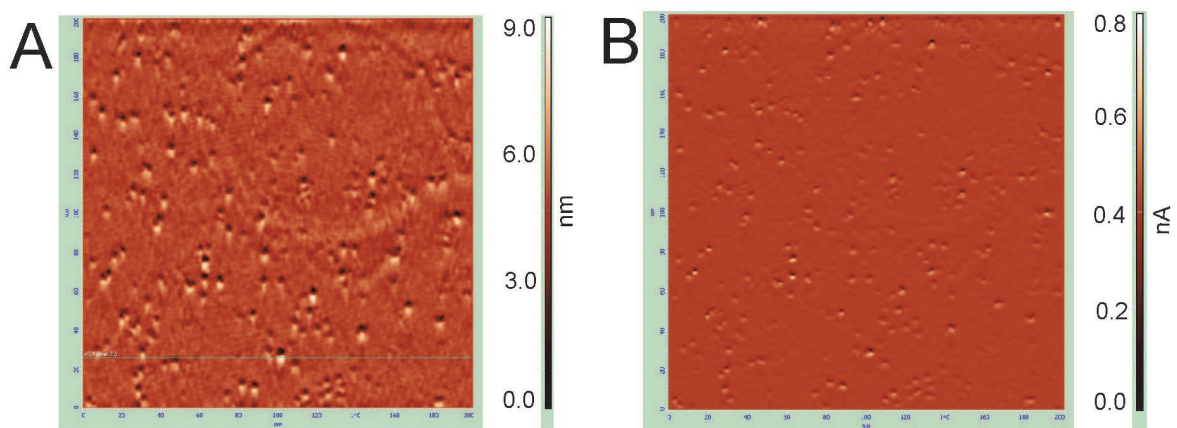


Fig. 9. $200 \times 200 \text{ nm}^2$ scan of HOPG substrate with electrodeposited Au nanoparticles due to PLA+EPD process while $17 \mu\text{A}$ passed through ethanolic ablation medium: (A) Topography, (B) tunnelling current image.

Therefore, on the basis of these results, it can be concluded that the substrate roughness in the range of hundreds of nanometers (the case of FTO-coated glass substrate) distinctly impedes the homogeneous coverage of substrate by electrodeposited Au nanoparticles. On the contrary, the surface roughness being below 1 nm does not hamper a homogeneous distribution of electrodeposited Au nanoparticles.

3.3 Possible elucidation of direct current value influence on mechanism of Au nanoparticles generation during PLA+EPD process in primary alcohols

Since *the final stages* of Au nanoparticles solutions and/or the electrodeposited Au nanoparticles on different substrates have been investigated, it cannot be unambiguously stated the exact formation mechanism of Au nanoparticles during the PLA+EPD process. However, it can be hypothesized the influence of direct current value on the mechanism of Au nanoparticles generation by the PLA+EPD process in comparison to a generally adopted mechanism of pulsed-laser ablation itself.

The prevailing formation mechanism of nanoparticles by a classical pulsed-laser ablation process implies the generation of a plasma plume followed by its cooling (Amendola & Meneghetti, 2009; Tsuji et al., 2004). The former step is nothing else than the vaporization of the part of a target which was attacked by the focused beam of laser pulses. During the second step (plasma plume cooling), the formation of nanoparticles nuclei starts. The driving force for the nucleation is the supersaturation in the plasma plume (Amendola & Meneghetti, 2009). Subsequently, the nuclei grow and coalesce into the sizes of resulting nanoparticles. This last step strongly depends on the polarity of solvents, the presence and/or the absence of simple ions or adsorbing species which may stabilize nanoparticles of a particular size.

Under the assumption that our pulsed-laser ablation process in the selected solvent (e.g. ethanol or butanol) is repeatedly performed in the same way and under otherwise the same experimental conditions, the value of the applied electric field can induce changes rather in the step of nuclei growth and coalescence than during the plasma plume generation and/or the nucleation process. As it has been pointed out in section 3.1, ethanol possesses a higher dielectric constant than butanol which means that ethanol is more easily polarized by an increasing electric field than butanol. This implies that a further nuclei growth and coalescence is possibly hindered in the case of 17 μA direct current value passing through the ethanolic ablation medium when pulsed-laser ablation takes place. Basically, charged nanoparticles of smaller sizes in diameter can be efficiently stabilized in a more polarized solvent, i.e., in our case, at a higher current value passing through the ethanolic ablation medium. Thus, a smaller average particle size is observed in Au17 than in Au10 solutions. Nevertheless, this hypothesis needs a further experimental support which is beyond the scope of this chapter.

4. Conclusions

The application of nanosecond laser pulses of 532 nm laser wavelength for the generation of Au nanoparticles in primary alcohols (ethanol and butanol) has been discussed and the impact of a direct current passing simultaneously through the ablation medium during the pulsed-laser ablation process has been determined. On the basis of a complete characterization of Au nanoparticles solutions, it has been concluded that the average size of

Au nanoparticles can be influenced by the type of an alcoholic ablation medium as well as by the direct current value (the latter induces changes only in the case of ethanol). Moreover, the length of aliphatic chains in the two selected alcohols affects the character of coverage of ITO-coated glass substrates by Au nanoparticles; more evenly dispersed electrodeposited Au nanoparticles have been encountered in the butanolic ablation medium. In contrast, aggregates of Au nanoparticles have been observed when the ethanolic ablation medium used. The amount of electrodeposited Au nanoparticles is generally higher in ethanol than in butanol which can be related to the differences in zeta potential values of Au nanoparticles. The surface roughness of substrates has appeared to be another very important parameter influencing the final characteristic coverage of substrates by Au nanoparticles generated by the PLA+EPD process. An excellent correlation between microscopic and spectroscopic results has been demonstrated. Finally, a possible explanation of the influence of direct current value on the mechanism of Au nanoparticles generation during the PLA+EPD process has been proposed.

5. Acknowledgment

The author thanks to Mrs. Jiřina Hromádková for SEM and TEM imaging. Financial support by GAČR P108/11/P657 is gratefully acknowledged.

6. References

- Amendola, V., Rizzi, G.A., Polizzi, S. & Meneghetti, M. (2005). Synthesis of gold nanoparticles by laser ablation in toluene: quenching and recovery of the surface plasmon absorption. *The Journal of Physical Chemistry B*, Vol. 109, No. 49, pp. 23125-23128, ISSN 1520-6106 print / ISSN 1520-5207 online
- Amendola, V., Polizzi, S. & Meneghetti, M. (2007). Free silver nanoparticles synthesized by laser ablation in organic solvents and their easy functionalization. *Langmuir*, Vol. 23, No. 12, pp. 6766-6770, ISSN 0743-7463 print / ISSN 1520-5827 online
- Amendola, V. & Meneghetti, M. (2009). Laser ablation synthesis in solution and size manipulation of noble metal nanoparticles. *Physical Chemistry Chemical Physics*, Vol. 11, pp. 3805-3821, ISSN 1463-9076 print / ISSN 1463-9084 online
- Atwater, H.A. & Polman A. (2010). Plasmonics for improved photovoltaic devices. *Nature Materials*, Vol. 9, pp. 205-213, ISSN 1476-1122 print / ISSN 1476-4660 online
- Boyer, P., Menard, D. & Meunier, M. (2010). Nanoclustered Co-Au particles fabricated by femtosecond laser fragmentation in liquids. *J. Phys. Chem. C*, Vol. 114, No. 32, pp. 13497-13500, ISSN 1932-7447 print / ISSN 1932-7455 online
- Buining, PA, Humbel, BM, Phillipse, AP & Verkleij, AJ. (1997). Preparation of functional silane-stabilized gold colloids in the (sub)nanometer size range. *Langmuir*, Vol. 13, No. 15, pp. 3921-3926, ISSN 0743-7463 print / ISSN 1520-5827 online
- Burakov, V.S., Tarasenko, N.V., Butsen, A.V., Rozantsev, V.A. & Nedelko, M.I. (2005). Formation of nanoparticles during double-pulse laser ablation of metals in liquids. *Eur. Phys. J. Appl. Phys.*, Vol. 30, pp. 107-112, ISSN 0021-8979 print / ISSN 1089-7550 online

- Burakov, V.S., Butsen, A.V. & Tarasenko, N.V. (2010). Laser-induced plasmas in liquids for nanoparticle synthesis. *Journal of Applied Spectroscopy*, Vol. 77, No. 3, pp. 386-393, ISSN 0021-9037 print / ISSN 1573-8647 online
- Carrara, M., Kakkassery, J.J., Abid, J.P. & Fermin, D.J. (2004). Modulation of the work function in layer-by-layer assembly of metal nanoparticles and poly-L-lysine on modified Au surfaces. *Chem. Phys. Chem.*, Vol. 5, pp. 571-575, ISSN 1439-7641
- Compagninni, G., Scalisi, A.A. & Puglisi, O. (2002). Ablation of noble metals in liquids: a method to obtain nanoparticles in a thin polymeric film. *Phys. Chem. Chem. Phys.*, Vol. 4, pp. 2787-2791, ISSN 1463-9076 print / ISSN 1463-9084 online
- Dammer, O., Vlckova, B., Slouf, M. & Pflieger, J. (2007). Interaction of high-power laser pulses with monodisperse gold particles. *Materials Science and Engineering B*, Vol. 140, pp. 138-146, ISSN 0921-5107
- Darroudi, M., Ahmad, M. B., Zamiri, R., Abdullah, A.H., Ibrahim, N.A., Shameli, K. & Husin, M.S. (2011). Preparation and characterization of gelatine mediated silver nanoparticles by laser ablation. *Journal of Alloys and Compounds*, Vol. 509, pp. 1301-1304, ISSN 0925-8388
- de Boer, B., Hadipour, A., Mandoc, M.M., van Woudenberg, T. & Blom, P.W.M. (2005). Tuning of metal work functions with self-assembled monolayers. *Adv.Mater.*, Vol. 17, No. 5, pp. 621-625, ISSN 0935-9648 print / ISSN 1521-4095 online
- Doron, A., Katz, E. & Willner, I. (1995). Organization of Au colloids as monolayer films onto ITO glass surfaces: application of the metal colloid films as base interfaces to construct redox-active monolayers. *Langmuir*, Vol. 11, No. 4, 1313-1317, ISSN 0743-7463 print / ISSN 1520-5827 online
- Durston, P.J., Palmer, R.E. & Wilcoxon, J.P. (1998). Manipulation of passivated gold clusters on graphite with the scanning tunneling microscope. *Appl. Phys. Lett.*, Vol. 72, No. 2, pp. 176-178, ISSN 0003-6951 print / ISSN 1077-3118 online
- Fong, Y.Y., Gascooke, J. R., Visser, B.R., Metha, G.F. & Buntine, M.A. (2010). Laser-based formation and properties of gold nanoparticles in aqueous solution: formation kinetics and surfactant-modified particle size distributions. *J. Phys. Chem. C*, Vol. 114, No. 38, pp. 15931-15940, ISSN 1932-7447 print / ISSN 1932-7455 online
- Franklin, S.R. & Thareja, R.K. (2004). Simplified model to account for dependence of ablation parameters on temperature and phase of the ablated material. *Applied Surface Science*, Vol. 222, pp. 293-306, ISSN 0169-4332
- Georgiou, S. & Koubenakis, A. (2003). Laser-induced material ejection from model molecular solids and liquids: mechanisms, implications, and applications. *Chemical Reviews*, Vol. 103, No. 2, pp.349-393, ISSN 0009-2665 print / ISSN 1520-6890 online
- Grabar, K.C., Allison, K.J., Baker, B.E., Bright, R.M., Brown, K.R., Freeman, R.G., Fox, A.P., Keating, Ch.D., Musick, M.D. & Natan, M.J. (1996). Two-dimensional arrays of colloidal gold particles: a flexible approach to macroscopic metal surfaces. *Langmuir*, Vol. 12, No. 10, 2353-2361, ISSN 0743-7463 print / ISSN 1520-5827 online
- Grzelczak, M., Vermant, J., Furst, E.M. & Liz-Marzan, L.M. (2010). Directed self-assembly of nanoparticles. *ACS Nano*, Vol. 4, No. 7, pp. 3591-3605, ISSN 1936-0851 print / ISSN 1936-086X online

- He, H., Cai, W., Lin, Y. & Chen, B. Surface decoration of ZnO nanorod arrays by electrophoresis in the Au colloidal solution prepared by laser ablation in water. *Langmuir*, Vol. 26, No. 11, 8925-8932, ISSN 0743-7463 print / ISSN 1520-5827 online
- Inasawa, S., Sugiyama, M., Noda, S. & Yamaguchi, Y. (2006). Spectroscopic study of laser-induced phase transition of gold nanoparticles on nanosecond time scales and longer. *J. Phys. Chem. B*, Vol. 110, No. 7, pp. 3114-3119, ISSN 1520-6106 print / ISSN 1520-5207 online
- Jain, P.K., El-Sayed, I.H. & El-Sayed M.A. (2007). Au nanoparticles target cancer. *Nanotoday*, Vol. 2, No. 1, pp. 18-28, ISSN 1748-0132
- Kabashin, A.V., Meunier, M., Kingston, Ch. & Luong, J.H.T. (2003). Fabrication and characterization of gold nanoparticles by femtosecond laser ablation in an aqueous solution of cyclodextrins. *J. Phys. Chem. B*, Vol. 107, No. 19, pp. 4527-4531, ISSN 1520-6106 print / ISSN 1520-5207 online
- Kamat, P.V., Flumiani, M. & Hartland, G.V. (1998). Picosecond dynamics of silver nanoclusters. Photoejection of electrons and fragmentation. *J. Phys. Chem. B*, Vol. 102, No. 17, pp. 3123-3128, ISSN 1520-6106 print / ISSN 1520-5207 online
- Kim, S.S., Na, S.I., Kim, D.Y. & Nah, Y.Ch. (2008). Plasmon enhanced performance of organic solar cells using electrodeposited Ag nanoparticles. *Appl. Phys. Lett.*, Vol. 93, 073307, ISSN 0003-6951 print / ISSN 1077-3118 online
- Kurita, H., Takami, A. & Koda, S. (1998). Size reduction of gold particles in aqueous solution by pulsed laser. *Appl. Phys. Lett.*, vol. 72, No. 7, pp. 789-791, ISSN 0003-6951 print / ISSN 1077-3118 online
- Le Ru, E. & Etchegoin, P. (2008). *Principles of Surface-Enhanced Raman Spectroscopy and related plasmonic effects*, Elsevier Science, ISBN 0444527796, Amsterdam, The Netherlands
- Link, S., Burda, C. Mohamed, M.B., Nikoobakht, B. & El-Sayed, M.A. (1999). Laser photothermal melting and fragmentation of gold nanorods: energy and laser pulse-width dependence. *J. Phys. Chem. A*, Vol. 103, No. 9, pp. 1165-1170, ISSN 1089-5639 print / ISSN 1520-5215 online
- Link, S & El-Sayed, MA. (2003). Optical properties and ultrafast dynamics in metallic nanocrystals. *Annu. Rev. Phys. Chem.*, Vol. 54, pp. 331-366, ISSN 0066-426X
- Mafune, F., Kohno, Jy., Takeda, Y. & Kondow, T. (2001). Dissociation and aggregation of gold nanoparticles under laser irradiation. *J. Phys. Chem. B*, Vol. 105, No. 38, pp. 9050-9056, ISSN 1520-6106 print / ISSN 1520-5207 online
- Mafune, F., Kohno, Jy., Takeda, Y. & Kondow, T. (2002). Full physical preparation of sized-selected gold nanoparticles in solution: laser ablation and laser-induced size control. *J. Phys. Chem. B*, Vol. 106, No. 31, pp. 7575-7577, ISSN 1520-6106 print / ISSN 1520-5207 online
- Menendez-Manjon, A., Jakobi, J., Schwabe, K., Krauss, J.K. & Barcikowski, S. (2009). Mobility of nanoparticles generated by femtosecond laser ablation in liquids and its application to surface patterning. *JLMN-Journal of Laser Micro/Nanoengineering*, Vol. 4, No. 2, pp. 95-99, ISSN 1880-0688
- Morfa, A.J., Rowlen, K.L., Reilly III, T.H., Romero, M.J. & van de Lagemaat, J. (2008). Plasmon-enhanced solar energy conversion in organic bulk heterojunction

- photovoltaics. *Appl. Phys. Lett.*, Vol. 92, 013504, ISSN 0003-6951 print / ISSN 1077-3118 online
- Mortier, T., Verbiest, T. & Persoons, A. (2003). Laser ablation of gold in chloroform solutions of cetyltrimethylammoniumbromide. *Chem.Phys.Lett.*, Vol. 382, pp. 650-653, ISSN 0009-2614
- Muto, H., Yamada, K., Miyajima, K. & Mafune, F. (2007). Estimation of surface oxide on surfactant-free gold nanoparticles laser-ablated in water. *J.Phys.Chem. C*, Vol. 111, No. 46, pp. 17221-17226, ISSN 1932-7447 print / ISSN 1932-7455 online
- Nah, Y.Ch., Kim, S.S., Park, J.H. & Kim, D.Y. (2007). Electrochromic coloration of MEH-PPV films by electrodeposited Au nanoparticles. *Electrochemical and Solid-State Letters*, Vol. 10, No. 1, pp. J12-J14, ISSN 1099-0062
- Peng, Z., Walther, T. & Kleinermanns, K. (2005). Photofragmentation of phase-transferred gold nanoparticles by intense pulsed laser light. *J.Phys.Chem.B*, Vol. 109, No. 33, pp. 15735-15740, ISSN 1520-6106 print / ISSN 1520-5207 online
- Procházka, M., Mojzeš, M., Štěpánek, J., Vlčková, B. & Turpin, P.Y. (1997). Probing applications of laser-ablated Ag colloids in SERS spectroscopy: improvement of ablation procedure and SERS spectral testing. *Anal. Chem.*, Vol. 69, No. 24, pp. 5103-5108, ISSN 0003-2700 print / ISSN 1520-6882 online
- Roduner, E. (2006). *Nanosopic Materials: Size-dependent Phenomena*, The Royal Society of Chemistry, ISBN-13: 978-0-85404-857-1, Dorchester, Dorset, UK
- Semerok, A., Chaleard, C., Detalle, V., Lacour, J.L., Mauchien, P., Meynadier, P., Nouvellon, C., Salle, B., Palianov, P., Perdrix, M. & Petite, G. (1999). Experimental investigations of laser ablation efficiency of pure metals with femto, pico and nanosecond pulses. *Applied Surface Science*, Vol. 138-139, pp. 311-314, ISSN 0169-4332
- Shoji, M., Miyajima, K. & Mafune, F. (2008). Ionization of gold nanoparticles in solution by pulse laser excitation as studied by mass spectrometric detection of gold cluster ions. *J. Phys. Chem. C*, Vol. 112, No. 6, pp. 1929-1932, ISSN 1932-7447 print / ISSN 1932-7455 online
- Simakin, A.V., Voronov, V.V., Kirichenko, N.A. & Shafeev, G.A. (2004). Nanoparticles produced by laser ablation of solids in liquid environment. *Appl. Phys. A*, Vol. 79, pp. 1127-1132, ISSN 0947-8396 print / ISSN 1432-0630 online
- Sládková, M., Vlčková, B., Mojzeš, P., Šlouf, M., Naudin & C. LeBourdon, G. (2006). Probing strong optical fields in compact aggregates of silver nanoparticles by SERRS of protoporphyrin IX. *Faraday Discuss.*, Vol. 132, pp. 121-134, ISSN 0301-7249 print / ISSN 1364-5498 online
- Sobhan, MA, Ams, M, Withford, MJ & Goldys, EM. (2010). Ultrafast laser ablative generation of gold nanoparticles: the influence of pulse energy, repetition frequency and spot size. *J. Nanopart. Res.*, Vol. 12, pp. 2831-2842, ISSN 1388-0764 print / ISSN 1572-896X online
- Srnová, I., Procházka, M., Vlčková, B., Štěpánek, J. & Malý, P. (1998). Surface-enhanced Raman scattering-active systems prepared from Ag colloids laser-ablated in chemically modified aqueous media. *Langmuir*, Vol. 14, No. 16, 4666-4670, ISSN 0743-7463 print / ISSN 1520-5827 online

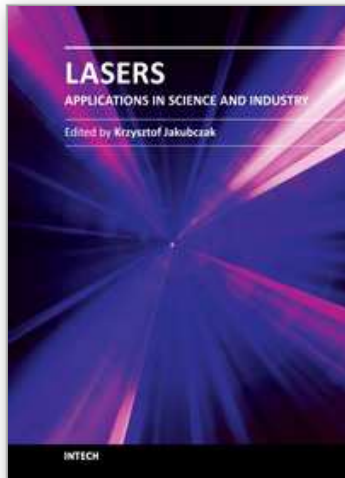
- Sýkora, V. (1976). *Chemicko-analytické tabulky*. SNTL, ISBN 80-03-00049-1, Prague, Czech Republic
- Sylvestre, J.P., Poulin, S., Kabashin, A.V., Sacher, E., Meunier, M. & Luong, J.H.T. (2004). Surface chemistry of gold nanoparticles produced by laser ablation in aqueous media. *J.Phys.Chem. B*, Vol. 108, pp. 16864-16869, ISSN 1520-6106 print / ISSN 1520-5207 online
- Rabani, E., Reichman, D.R., Geissler, P.L. & Brus, L.E. (2003). Drying-mediated self-assembly of nanoparticles *Nature*, vol. 426, pp. 271-274, , ISSN 1545-0740
- Rotello, V. (Ed.). (2004). *Nanoparticles: Building blocks for nanotechnology*. Kluwer Academi/Plenum Publishers, ISBN 0-306-48287-8, New York, USA
- Schnippering, M., Carrara, M., Foelske, A., Kotz, R. & Fermin, D.J. (2007). Electronic properties of Ag nanoparticle arrays. A Kelvin probe and high resolution XPS study. *Phys.Chem.Chem.Phys.*, Vol. 9, pp. 725-730, ISSN 1463-9076 print / ISSN 1463-9084 online
- Šišková, K., Vlčková, B., Turpin, P.Y., Fayet, C. Hromádková, J. & Šlouf, M. (2007). Effect of citrate ions on laser ablation of Ag foil in aqueous medium. *Journal of Physics: Conference Series*, Vol. 59, pp. 202-205, ISSN 1742-6588 print / ISSN 1742-6596 online
- Šišková, K., Vlčková, B., Turpin, P.Y., Thorel, A. & Grosjean, A. (2008). Porphyrins as SERRS spectral probes of chemically functionalized Ag nanoparticles. *Vibrational Spectroscopy*, Vol. 48, pp. 44-52, ISSN 0924-2031
- Šišková, K., Pflieger, J. & Procházka, M. (2010). Stabilization of Au nanoparticles prepared by laser ablation in chloroform with free-base porphyrin molecules. *Applied Surface Science*, Vol. 256, pp. 2979-2987, ISSN 0169-4332
- Šišková, K., Vlčková, B., Turpin, P.Y., Thorel, A. & Procházka, M. (2011). Laser ablation of silver in aqueous solutions of organic species: probing Ag nanoparticle-adsorbate systems evolution by surface-enhanced Raman and surface plasmon extinction spectra. *J. Phys. Chem. C*, Vol. 115, pp. 5404-5412, ISSN 1932-7447 print / ISSN 1932-7455 online
- Šišková, K., Šafářová, K., Seo, J.H., Zbořil, R. & Mashlan, M. (2011) Non-chemical approach toward 2D self-assemblies of Ag nanoparticles via cold plasma treatment of substrates. *Nanotechnology*, Vol. 22, 275601 (7pp) NANO/381585/PAP, ISSN 0957-4484 print / ISSN 1361-6528 online
- Šloufová-Srnová, I. & Vlčková, B. (2002) Two-dimensional assembling of Au nanoparticles mediated by tetrapyridylporphine molecules. *NanoLetters*, Vol. 2, No. 2, 121-125, ISSN 1530-6984 print / ISSN 1530-6992 online
- Šmejkal, P., Šišková, K., Vlčková, B., Pflieger, J., Šloufová, I., Šlouf, M. & Mojžeš, P. (2003). Characterization and surface-enhanced Raman spectral probing of silver hydrosols prepared by two-wavelength laser ablation and fragmentation. *Spectrochimica Acta A*, Vol. 59, pp. 2321-2329, ISSN 1386-1425
- Šmejkal, P., Pflieger, J., Šišková, K., Vlčková, B., Dammer, O. & Šlouf, M. (2004). In-situ study of Ag nanoparticle hydrosol optical spectra evolution during laser ablation/fragmentation. *Appl. Phys. A*, Vol. 79, pp. 1307-1309, ISSN 0947-8396 print / ISSN 1432-0630 online

- Takami, A., Kurita, H. & Koda, S. (1999). Laser-induced size reduction of noble metal particles. *J.Phys.Chem.B*, Vol. 103, No. 8, pp. 1226-1232, ISSN 1520-6106 print / ISSN 1520-5207 online
- Takeda, Y., Kondow, T. & Mafune, F. (2005). Formation of Au(III)-DNA coordinate complex by laser ablation of Au nanoparticles in solution. *Nucleoside, Nucleotides, and Nucleic Acids*, Vol. 24, No. 8, pp. 1215-1225, ISSN 1525-7770 print / 1532-2335 online
- Tarasenko, N.V., Butsen, A.V. & Nevar, E.A.(2005). Laser-induced modification of metal nanoparticles formed by laser ablation technique in liquids. *Applied Surface Science*, Vol. 247, pp. 418-422, ISSN 0169-4332
- Tsuji, T., Tsuboi, Y., Kitamura, N. & Tsuji, M. (2004). Microsecond-resolved imaging of laser ablation at solid-liquid interface: investigation of formation process of nano-size metal colloids. *Applied Surface Science*, Vol. 229, pp. 365-371, ISSN 0169-4332
- Tsuji, T., Mizuki, T., Yasutomo, M., Tsuji, M., Kawasaki, H., Yonezawa, T. & Mafune, F. (2011). Efficient fabrication of substrates for surface-assisted laser desorption/ionization mass spectrometry using laser ablation in liquids. *Applied Surface Science*, Vol. 257, pp. 2046-2050, ISSN 0169-4332
- Wang, B., Xiao, X., Huang, X., Sheng, P. & Hou, J.G. (2000). Single-electron tunneling study of two-dimensional gold clusters. *Appl.Phys.Lett.*, Vol. 77, No. 8, pp. 1179-1181, ISSN 0003-6951 print / ISSN 1077-3118 online
- Wender, D., Andrezza, M.L., Correia, R.R.B., Teixeira, S.R. & Dupont, J. (2011). Synthesis of gold nanoparticles by laser ablation of an Au foil inside and outside ionic liquids. *Nanoscale*, Vol. 3, pp. 1240-1245, ISSN 2040-3364 print + online / ISSN 2040-3372 online only
- Werner, D., Hashimoto, S., Tomita, T., Matsuo, S. & Makita, Y. (2008). Examination of silver nanoparticle fabrication by pulsed-laser ablation of flakes in primary alcohols. *J.Phys. Chem. C*, Vol. 112, No. 5, pp. 1321-1329, ISSN 1932-7447 print / ISSN 1932-7455 online
- Werner, D., Hashimoto, S. & Uwada, T. (2010). Remarkable photothermal effect of interband excitation on nanosecond laser-induced reshaping and size reduction of pseudospherical gold nanoparticles in aqueous solution. *Langmuir*, Vol. 26, No. 12, pp. 9956-9963, ISSN 0743-7463 print / ISSN 1520-5827 online
- Wu, K.Y., Yu, S.Y. & Tao, Y.T. (2009). Continuous modulation of electrode work function with mixed self-assembled monolayers and its effect in charge injection. *Langmuir*, Vol. 25, No.11, pp. 6232-6238, ISSN 0743-7463 print / ISSN 1520-5827 online
- Yamada, K., Tokumoto, Y., Nagata, T. & Mafune, F. (2006). Mechanism of laser-induced size-reduction of gold nanoparticles as studied by nanosecond transient absorption spectroscopy. *J. Phys. Chem. B*, Vol. 110, No. 24, pp. 11751-11756, ISSN 1520-6106 print / ISSN 1520-5207 online
- Yamada, K., Miyajima, K. & Mafune, F. (2007). Thermionic emission of electrons from gold nanoparticles by nanosecond pulse-laser excitation of interband. *J. Phys. Chem. C*, Vol. 111, No. 30, pp. 11246-11251, ISSN 1932-7447 print / ISSN 1932-7455 online
- Yang, S., Cai, W., Liu, G. & Zeng, H. (2009). From nanoparticles to nanoplates: preferential oriented connection of Ag colloids during electrophoretic deposition. *J. Phys. Chem. C*, Vol. 113, No. 18, 7692-7696, ISSN 1932-7447 print / ISSN 1932-7455 online

- Zhigilei, L.V. & Garrison, B.J. (1999). Mechanisms of laser ablation from molecular dynamics simulations: dependence of the initial temperature and pulse duration. *Appl.Phys.A*, Vol. 69, pp. S75-S80, ISSN 0947-8396 print / ISSN 1432-0630 online
- Zhitomirsky, I., Petric, A. & Niewczas, M. (2002). Nanostructured ceramic and hybrid materials via electrodeposition. *JOM*, Vol. September, pp. 31-35, ISSN 1047-4838 print / ISSN 1543-1851 online

IntechOpen

IntechOpen



Lasers - Applications in Science and Industry

Edited by Dr Krzysztof Jakubczak

ISBN 978-953-307-755-0

Hard cover, 276 pages

Publisher InTech

Published online 09, December, 2011

Published in print edition December, 2011

The book starts with basic overview of physical phenomena on laser-matter interaction. Then it is followed by presentation of a number of laser applications in the nano-particles and thin films production, materials examination for industry, biological applications (in-vitro fertilization, tissue ablation) and long-range detection issues by LIDARs.

How to reference

In order to correctly reference this scholarly work, feel free to copy and paste the following:

Karoľina Šiškova (2011). Pulsed-Laser Ablation of Au Foil in Primary Alcohols Influenced by Direct Current, Lasers - Applications in Science and Industry, Dr Krzysztof Jakubczak (Ed.), ISBN: 978-953-307-755-0, InTech, Available from: <http://www.intechopen.com/books/lasers-applications-in-science-and-industry/pulsed-laser-ablation-of-au-foil-in-primary-alcohols-influenced-by-direct-current>

INTECH
open science | open minds

InTech Europe

University Campus STeP Ri
Slavka Krautzeka 83/A
51000 Rijeka, Croatia
Phone: +385 (51) 770 447
Fax: +385 (51) 686 166
www.intechopen.com

InTech China

Unit 405, Office Block, Hotel Equatorial Shanghai
No.65, Yan An Road (West), Shanghai, 200040, China
中国上海市延安西路65号上海国际贵都大饭店办公楼405单元
Phone: +86-21-62489820
Fax: +86-21-62489821

© 2011 The Author(s). Licensee IntechOpen. This is an open access article distributed under the terms of the [Creative Commons Attribution 3.0 License](#), which permits unrestricted use, distribution, and reproduction in any medium, provided the original work is properly cited.

IntechOpen

IntechOpen